USE OF ALOS DATA FOR MONITORING CORAL REEF BLEACHING

PI No 204

Hiroya Yamano [1], Masayuki Tamura [2], Hajime Kayanne [3]

[1] National Institute for Environmental Studies, 16-2 Onogawa, Tsukuba, Ibaraki 305-8506, Japan
[2] Department of Urban and Environmental Engineering, Kyoto University, Katsura, Saikyo-ku, Kyoto 615-8540, Japan
[3] Department of Earth and Planetary Science, The University of Tokyo, 7-3-1 Hongo, Bunkyo, Tokyo 113-0033, Japan

1. INTRODUCTION

Coral reef bleaching is a major scientific and environmental issue [1, 2]. Bleaching frequency has increased since the early 1980s, and a severe global bleaching event took place in 1997 and 1998. One possible reason for the increased frequency of bleaching might be related to high sea-surface temperatures (SST) caused by global warming [3].

The loss in pigmented zooxanthellae from corals during bleaching events results in an optical signal that is strong enough for remote sensing to detect. Although global SST is monitored by the NOAA AVHRR sensor [4], studies on coral bleaching are based on in situ data [5] and aerial photography [6] at a relatively small spatial scale. Satellite remote sensing should be investigated, because satellite sensors can routinely obtain data on coral reefs on a large spatial scale of ca. 100 km x 100 km.

To examine the applicability of satellite remote sensing to coral reef assessment, we have conducted on research as follows

- We measured reflectance spectra of healthy and bleached corals, as well as other benthic features.
- We performed radiative transfer simulation to examine the feasibility of satellite remote sensing to detect bleaching.
- We analyzed satellite data to detect bleaching and changes due to bleaching

As a result we showed feasibility of using ALOS AVNIR2 to detect and monitor coral reef bleaching.

2. REFLECTANCE SPECTRA

Montipora digitata coral were collected from the reef around Sesoko Island, Japan on 24 August 2001. Three colonies that were visually recognized as pigmented corals were collected, at depths of 1-2 m. In addition, two M. digitata colonies that had been naturally bleached as a result of high sea surface temperatures were collected from the same reef.

The reflectance spectra of the coral specimens were measured under natural light between 10:30 and 11:00 A.M. For each reflectance measurement, the samples were transported to a flume lined with black fabric to minimize wall effects on the light field. We used FieldSpec Fr (Analytical Spectral Devices, Inc., USA) to measure the reflectance spectra at 1-nm intervals, using an attachment that enabled a 5-degree field of view. We measured the upwelling radiance in water from a white reference panel and then from a coral specimen soon after the reference measurement. The spectra were measured about 10 cm above the reference panel and above the corals in order to cover a circle 0.9 cm in diameter, which is within the width of a coral branch. The view zenith angle of the sensor was set to 0 degrees. The measurement was repeated 40 times for each specimen. The measurements of radiance were expressed as the ratio of the radiance of the coral to that of the reference panel, and average coral reflectance spectra were obtained. We also collected other spectra from previous publications [7].

The reflectance of healthy corals showed values similar to those of common brown-colored corals previously reported [8]. In contrast, the reflectance of bleached corals was significantly higher than previously reported [5, 9]. Of greatest importance is the absence of absorption in the red region, which indicates the loss of zooxanthellae. The bleached coral measured here still contained 1.1×10^4 healthy zooxanthellae per cm^2, but this number was 1/100 of the number of the healthy coral measured [10]. The bleached coral is regarded here as a still-living coral that has lost almost all of its symbionts. The data of the bleached corals show the maximum reflectance of bleached coral, and so are useful for examining the satellite remote sensing detection limits for bleached coral. This significantly higher reflectance values of bleached coral encourages the used of satellite sensors to detect bleaching.

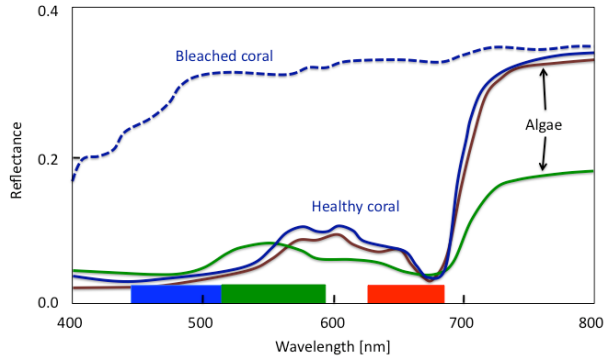

Fig. 1 Reflectance spectra of healthy and bleached corals. Spectra for algae [7] are also shown.

3. RADIATIVE TRANSFER SIMULATION

We calculated the radiance at Landsat TM bands 1, 2 and 3 in the visible region [11]. Our simulation would be applied to ALOS AVNIR2 data because of similar band assignment to those of Landsat TM. Two radiative transfer models for calculating radiance were used: 6S [12] and Hydrolight [13]. 6S was used for calculating photon absorption and scattering in the atmosphere. Hydrolight was used for calculating reflectance at the sea surface and photon absorption and scattering in seawater. Hydrolight computes spectral radiance both within water bodies and as the radiance leaves water bodies, based on the invariant imbedding theory. The calculated radiance from the sand substratum agreed well with that recorded by Landsat TM, validating the use of these two models in a coral-reef environment [14].

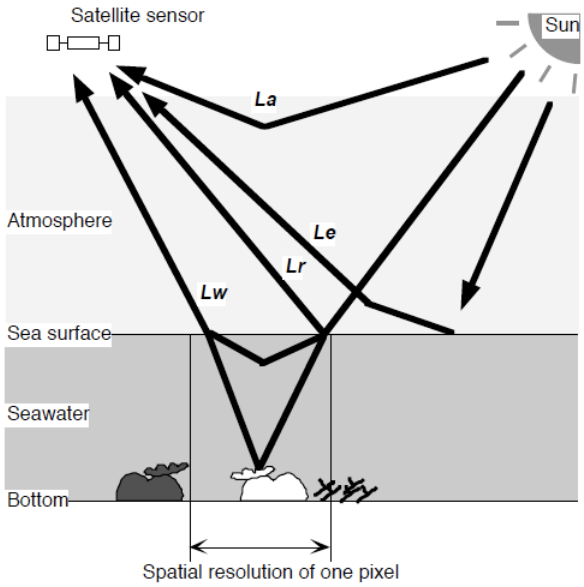

Fig. 2 Components of the radiance received by a satellite sensor for one pixel.

We calculated the radiance from bleached and healthy corals in order to examine the feasibility of using Landsat TM to detect coral reef bleaching. The basic parameters were prepared for the validation site, Ishigaki Island, Japan. We calculated the path radiance (*La* in Fig. 2), transmittance of the air, and incident light at the sea surface using 6S. Atmospheric condition was set to tropical type with a visibility of 40 km, and solar zenith angle was set to 25 degrees, considering the early- to mid-summer conditions at Ishigaki Island. Then, using Hydrolight, we calculated the radiance reflected from sea surface and the radiance from the bottom features by input of the values of incident light calculated by 6S. Wind speed was set to 0 m sec-1, as the wind has little effect on the irradiance reflectance at sea surface in the absence of foam and whitecaps for small solar zenith angles. Winds at the image acquisition time were less than 5 m sec^{-1}. We set chlorophyll a (Chl a) concentration to 0.5 mg m^{-3}, because the Chl a value range from 0.1 to 0.8 mg m^{-3} in the backreef lagoon of Ishigaki Island (Hata, personal communication). The scattering and absorption in the seawater volume were calculated according to Haltrin [15]. The radiance leaving the water was then multiplied by the direct transmittance of the air calculated by 6S, and the radiance (W m^{-2} sr^{-1} μm^{-1}) from the pixel of interest received by Landsat TM was obtained. We calculated the difference of the radiance before and after a bleaching event as a function of water depth and the difference in healthy coral coverage before and after the bleaching event.

The noise amplitudes (DN values) of TM bands 1, 2, and 3, which are critical for change detection, was estimated to be 2, 1, and 1 (standard deviations), respectively, based on the fluctuation of deep ocean values [14]. The difference in DN values needed to detect coral bleaching is assumed to be twice these values, or 4, 2 and 2, for bands 1, 2 and 3, respectively. Thus, the difference in radiance values calculated using Thome et al. [16] coefficients are 3.27, 3.06, and 2.25 W m^{-2} sr^{-1} μm^{-1}, respectively.

Fig. 3 shows the difference in DN values before and after a bleaching event as a function of water depth and the percentage of bleached corals in a TM pixel, which shows the difference in healthy coral coverage before and after the bleaching event. In this figure, we only showed a result for Band 1, but the same simulation was performed for bands 2 and 3. The detection limit of coral bleaching can be determined using Fig. 3. As described in the Methods section, it was assumed that coral bleaching could be detected if the difference in DN values was in excess of twice the error magnitude due to Landsat TM sensor noise. If a severe bleaching event occurred in an area that initially had an abundance of healthy corals (an area with an initial coral coverage of 100%, but in which all corals became completely bleached), the maximum

detectable depths were 28, 21, and 3.0 m for bands 1, 2 and 3, respectively. The vertical lines in Fig. 3 indicate a depth of 3 m, which indicates the maximum depth of reef flats in general. If the DN values from a coral pixel between two images can be compared directly, then Landsat TM bands 1, 2 and 3 can detect, at a depth of 3 m, differences of 10%, 9% and 94%, respectively, in healthy coral coverage in a pixel on reef flats due to bleaching.

In analyzing satellite data, error propagation in the normalization procedure must be taken into consideration. The errors for Landsat TM bands 1, 2 and 3 after the normalization procedure ranged from 1.72 to 3.35, from 1.67 to 2.53, and from 0.56 to 2.18 in radiance (W m^{-2} sr^{-1} μm^{-1}), respectively. Thus, the difference in DN values used for bleaching detection should be 6.70, 5.06 and 4.36 for the respective bands, and we use these values hereafter for bleaching detection. Thus, if a severe bleaching event occurred in an area that initially had an abundance of healthy corals, the maximum detectable depths were 18, 17, and 1.7 m for bands 1, 2 and 3, respectively. On reef flats, a 23% difference and a 16% difference in healthy coral coverage in a pixel due to bleaching would be detected at a depth of 3 m using bands 1 and 2, respectively, of the Landsat TM (Fig. 3). Using band 3, the detection is limited to a shallow (1 ~ 2 m) part of the reef flat.

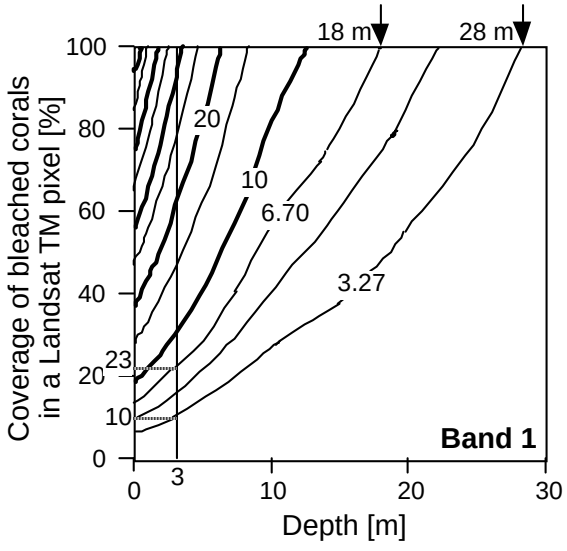

Fig. 3 Contours of calculated differences in radiance values for Landsat TM band 1 between bleached and healthy corals as a function of water depth and percent cover of bleached corals in a Landsat TM pixel. Vertical lines indicate the maximum depth of coral reef flats (3 m). Percentages show the minimum percent cover of bleached corals in a pixel detectable by Landsat TM, based both on the noise of the sensors only and on the propagation of errors in the Landsat TM data analysis.

4. SATELLITE DATA ANALYSIS

Landsat TM images (PATH 115, ROW 43) obtained from 1984 to 2000 were analyzed. These data include the image of 15 August 1998, when the severe bleaching event occurred. All of the images were georeferenced with rms errors smaller than 1.0. Only summer images were used, because bleaching is generally caused by the high SST under strong incident light from the higher solar elevation angles. In addition, the abundance of seaweed, whose reflectance spectra are similar to those of healthy coral, shows significant seasonal changes [17], a phenomenon that is also observed at Ishigaki Island. These characteristics would disturb the detection of coral reef bleaching in multitemporal data taken in different seasons.

We compared the DN from each pixel in the multitemporal images after removing the effects of path radiance, radiance from adjacent pixels, and the reflectance of seawater (Fig. 2), and then normalizing the effects of changes in the atmosphere, incident light, water depth and sensor response. The normalization procedure here was developed by Yamano and Tamura [11]. In this comparison, four assumptions were made: (1) the atmosphere is spatially uniform over a reef within a single image; (2) the incident light on the reef of interest is spatially uniform within an image; (3) the water quality (extinction coefficient) over the reef of interest is the same in any two images; and (4) the reflectance of sand and deep water are constant in any two images. To properly normalize each scene DN values from three types of substrate—shallow sand (DN_s), deep water (DN_d), and corals (DN_c)—are needed. These points should be as close as possible to each other spatially in order to reduce the possibility of local changes in atmospheric conditions and incident light due to the presence of clouds near the site. Furthermore, radiance from adjacent pixels (L_e in Fig. 2) is assumed to be the same for the three pixels, because the pixels are close to each other. The basic procedure is to compare the differences in DN values between sand (DN_s) and corals (DN_c) in multitemporal satellite images, after normalizing for changes in the atmosphere (transmittance), incident light, sensor characteristics, and water depth. If the value of (DN_s - DN_c) in one image is smaller than in other images, coral bleaching would be interpreted to have taken place, because DN_s should be constant and the DN_c value of bleached corals should be greater than that of healthy corals.

The digital number (DN_t) generated by a satellite sensor (Fig. 2) is a function of the radiance received at the sensor and is given for an individual pixel by

$$DN_t = G \cdot [L_w + L_r + L_e + L_a] + B \quad (1)$$

where G and B are the gain and offset values for converting the radiance to DN. In our work, the effect of multiple scattering in air and in seawater was ignored.

Radiance from the substrate is described as follows:

$$L_w = T \cdot Ed \cdot C \cdot \rho_b \cdot \exp[-2k \cdot z] \quad (2)$$

where T is light transmittance in air, Ed is downwelling irradiance above the sea surface within the given spectral band and the time of year and day when the image was collected, C is a factor that accounts for the loss of irradiance at the air-sea interface due to reflectance, ρ_b is the reflectance of bottom features, k is an extinction coefficient for water, and z is the water depth.

Consider the DN values from sand, deep water, and coral (DN_s, DN_d, and DN_c) in two images collected on different dates (images 1 and 2). Based on Eqs. 1 and 2, in the first image, the DN values are given by

$$DN_{s1} = G_1 \cdot [L_{s1} + L_{r1} + L_{e1} + L_{a1}] + B_1 \quad (3)$$

$$DN_{d1} = G_1 \cdot [L_{d1} + L_{r1} + L_{e1} + L_{a1}] + B_1 \quad (4)$$

$$DN_{c1} = G_1 \cdot [L_{c1} + L_{r1} + L_{e1} + L_{a1}] + B_1 \quad (5)$$

where

$$L_{s1} = T_1 \cdot Ed_1 \cdot C_1 \cdot \rho_{s1} \cdot \exp[-2k_1 \cdot z_{s1}] \quad (6)$$

$$L_{d1} = T_1 \cdot Ed_1 \cdot C_1 \cdot \rho_{d1} \cdot \exp[-2k_1 \cdot z_{d1}] \quad (7)$$

$$L_{c1} = T_1 \cdot Ed_1 \cdot C_1 \cdot \rho_{c1} \cdot \exp[-2k_1 \cdot z_{c1}] \quad (8)$$

In the second image, in which the water depth exceeds that of the first image by Δz due to tide, the DN values are given by

$$DN_{s2} = G_2 \cdot [L_{s2} + L_{r2} + L_{e2} + L_{a2}] + B_2 \quad (9)$$

$$DN_{d2} = G_2 \cdot [L_{d2} + L_{r2} + L_{e2} + L_{a2}] + B_2 \quad (10)$$

$$DN_{c2} = G_2 \cdot [L_{c2} + L_{r2} + L_{e2} + L_{a2}] + B_2 \quad (11)$$

where

$$L_{s2} = T_2 \cdot Ed_2 \cdot C_2 \cdot \rho_{s2} \cdot \exp[-2k_2 \cdot (z_{s1} + \Delta z)] \quad (12)$$

$$L_{d2} = T_2 \cdot Ed_2 \cdot C_2 \cdot \rho_{d2} \cdot \exp[-2k_2 \cdot (z_{d1} + \Delta z)] \quad (13)$$

$$L_{c2} = T_2 \cdot Ed_2 \cdot C_2 \cdot \rho_{c2} \cdot \exp[-2k_2 \cdot (z_{c1} + \Delta z)] \quad (14)$$

Here, $\rho_{s1} = \rho_{s2} = \rho_s$, $\rho_{d1} = \rho_{d2} = \rho_d$, and $k_1 = k_2 = k$, according to the assumptions described above.

The effects of adjacent pixels, path radiance, and the offset in converting the radiance to DN are removed by subtracting DN_c from DN_s in the same image.

$$DN_{s1} - DN_{c1} = G_1 \cdot T_1 \cdot Ed_1 \cdot C_1 \cdot [\rho_s \cdot \exp(-2k \cdot z_{s1}) - \rho_{c1} \cdot \exp(-2k \cdot z_{c1})] \quad (15)$$

$$DN_{s2} - DN_{c2} = G_2 \cdot T_2 \cdot Ed_2 \cdot C_2 \cdot [\rho_s \cdot \exp(-2k \cdot z_{s1}) - \rho_{c2} \cdot \exp(-2k \cdot z_{c1})] \exp[-2k \cdot \Delta z] \quad (16)$$

In order to perform the normalization between the images, (DN_{s1} - DN_{d1}) should be made to be equal to (DN_{s2} - DN_{d2}) by introducing a coefficient α:

$$\alpha = \frac{DN_{s1} - DN_{d1}}{DN_{s2} - DN_{d2}} = \frac{G_1 \cdot T_1 \cdot Ed_1 \cdot C_1}{G_2 \cdot T_2 \cdot Ed_2 \cdot C_2 \cdot \exp[-2k \cdot \Delta z]} \quad (17)$$

Thus, (DN_s - DN_c) in the second image (Eq. 16) is normalized with respect to the first image using α:

$$\alpha \cdot [DN_{s2} - DN_{c2}] = G_1 \cdot T_1 \cdot Ed_1 \cdot C_1 \cdot [\rho_s \cdot \exp(-2k \cdot z_{s1}) - \rho_{c2} \cdot \exp(-2k \cdot z_{c1})] \quad (18)$$

It can then be compared to Eq. 15 without knowledge of the atmospheric conditions or the difference in water depths due to tide between the two images, because the change in the DN value is produced only by the difference in coral reflectance (ρ_c).

The normalized values of (DN_s - DN_c) for Landsat TM bands 1 to 3 at 10 points in each image were compared with reference values of (DN_s − DN_d) from an image without clouds obtained on 16 May 1994, and the values were converted to radiance (W m^{-2} sr^{-1} μm^{-1}) using calibration coefficient for 1994 [16]. The propagation of errors due to Landsat TM sensor noise in the normalizing procedure was calculated. The calculated error magnitude was then used to estimate the detection limit for bleaching in the results of the radiative transfer simulation and the time-series satellite data analysis.

Fig. 4 shows the temporal changes of differences in radiance values between sand and corals at three validation sites with severe bleaching after applying the normalization procedure. The values of bands 1 and 2 at severely bleached sites were smallest in the summer of 1998. This corresponds to the severe bleaching event at the sites. The 1998 mass-bleaching event that produced 25 to 55% bleached coral cover would be detected by bands 1 and 2, as indicated by the radiative transfer simulation (see previous chapter). After 1997, the values of bands 1 and 2 decreased in June 1998 and reached their lowest values in August 1998, reflecting the progress of bleaching. The shallow water depth allowed band 3 to detect the 1998 bleaching event, which agrees well with the results of the radiative transfer simulation (see previous chapter).

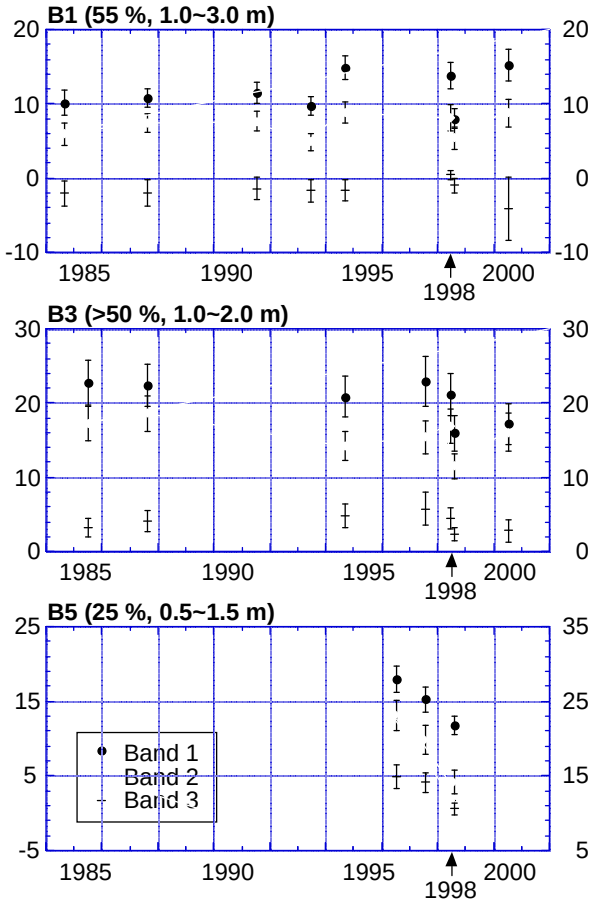

Fig. 4 Temporal changes in the difference of radiance from sand and from corals of Landsat TM bands 1 to 3 at severely bleached sites. Bars show errors (±1σ). Percent coverage of bleached corals and water depths at the site are indicated in parentheses.

In response to these results on Landsat TM, we performed analysis of ALOS AVNIR2 data to detect bleaching in 2007. After normalization procedure shown above, bleaching in the summer of 2007 appeared to be detected in Ishigaki Island by comparison of FORMOSAT and ALOS AVNIR2 data (Fig. 5).

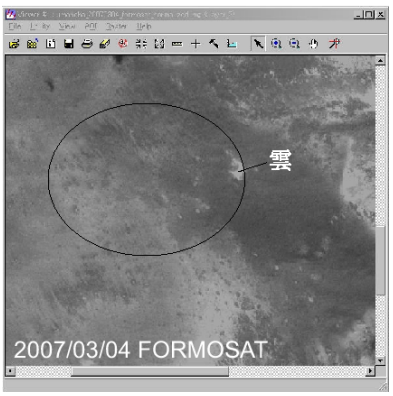

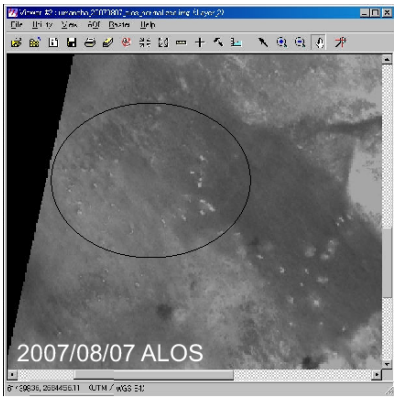

Fig. 5 FORMOSAT (upper) and ALOS AVNIR2 (lower) images in 2007. The ALOS AVNIR 2 image taken during bleaching showed white patches, suggesting detection of bleaching.

We further explored the possibility to detect long-term effect of bleaching. In Ishigaki Island, coral cover significantly decreased due to the 1998 bleaching. Because dead corals often show higher reflectance values, it could be possible to monitor coral die-off due to bleaching. A supervised classification of two satellite images before and after the 1998 bleaching (Landsat TM and ALOS AVNIR2) showed significant decline of coral reefs in Ishigaki Island (Fig. 6).

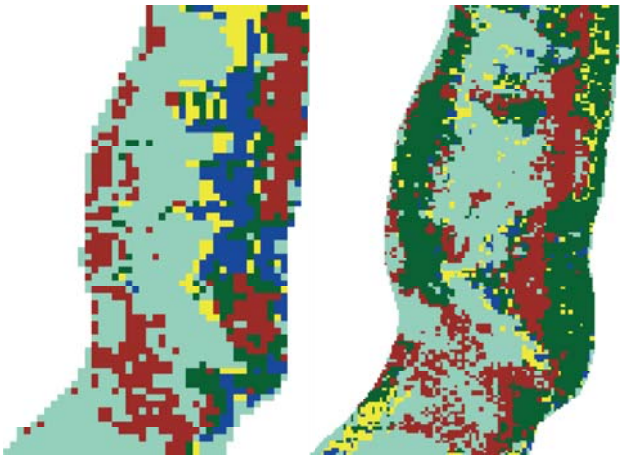

Fig. 6 Comparison of 1990 (left; Landsat TM) and 2006 (right; ALOS AVNIR2) images classified for Shirao Reef, Ishigaki Island. Blue area, which indicates high coral cover, significantly decreased in 2006, probably due to the bleaching in 1998.

5. CONCLUSIONS

In this project we have performed rigorous assessment of satellite data, including ALOS AVNIR2, for detecting

and monitoring coral bleaching. Results are summarized below.

- Reflectance spectra of bleached corals showed significantly higher reflectance values in comparison with other benthic features such as healthy corals and algae.
- Radiative transfer simulation showed that Landsat TM could detect bleaching that causes 23% difference in live coral cover.
- Time series satellite data, which were normalized for the effects on tide and atmosphere, enabled us to detect bleaching. Higher spatial resolution sensors (e.g., ALOS AVNIR2) would enhance the detection. A comparison between pre- and ongoing-bleaching images showed possible detection of bleaching by using ALOS AVNIR2.
- Mortality of corals due to bleaching could be also detected by satellite data (Landsat TM and ALOS AVNIR2) by using image classification technique.

These results serve as baselines for detecting and monitoring coral bleaching by satellite remote sensing.

6. REFERENCES

[1] P. W. Glynn, "Coral reef bleaching: ecological perspectives," *Coral Reefs*, vol. 12, pp. 1-17, 1993.

[2] B. E. Brown, "Coral bleaching: causes and consequences," *Coral Reefs*, vol. 16 (Suppl), pp. S129-S138, 1997.

[3] O. Hoegh-Guldberg, P. J. Mumby, A. J. Hooten *et al.*, "Coral reefs under rapid climate change and ocean acidification," *Science*, vol. 318, pp. 1737-1742, 2007.

[4] T. J. Goreau, and R. L. Hayes, "Coral bleaching and ocean "Hot Spots"," *Ambio*, vol. 23, pp. 176-180, 1994.

[5] H. Holden, and E. LeDrew, "Spectral discrimination of healthy and non-healthy corals based on cluster analysis, principal components analysis, and derivative spectroscopy," *Remote Sens. Environ.*, vol. 65, pp. 217-224, 1998.

[6] S. Andréfouët, R. Berklemans, L. Odrizola *et al.*, "Choosing the appropriate spatial resolution for monitoring coral bleaching events using remote sensing," *Coral Reefs*, vol. 21, pp. 147-154, 2002.

[7] S. Maritorena, A. Morel, and B. Gentitli, "Diffuse reflectance of oceanic shallow waters: influence of water depth and bottom albedo," *Limnol. Oceanogr.*, vol. 39, pp. 1689-1703, 1994.

[8] E. J. Hochberg, M. J. Atkinson, A. Apprill *et al.*, "Spectral reflectance of coral," *Coral Reefs*, vol. 23, pp. 84-95, 2004.

[9] E. J. Hochberg, and M. J. Atkinson, "Spectral discrimination of coral reef benthic communities," *Coral Reefs*, vol. 19, pp. 164-171, 2000.

[10] H. Yamano, M. Tamura, Y. Kunii *et al.*, "Spectral reflectance as a potential tool for detecting stressed corals," *Galaxea, JCRS*, vol. 5, pp. 1-10, 2003.

[11] H. Yamano, and M. Tamura, "Detection limits of coral reef bleaching by satellite remote sensing: simulation and data analysis," *Remote Sensing of Environment*, vol. 90, pp. 86-103, 2004.

[12] E. F. Vermote, D. Tanré, J. L. Deuzé *et al.*, *Second Simulation of the Satellite Signal in the Solar Spectrum (6S) User Guide*, Technical report, Laboratoire d'optique atmosphérique, Lille, France, 1996.

[13] C. D. Mobley, *Light and water: radiative transfer in natural waters*, London: Academic Press, 1994.

[14] H. Yamano, and M. Tamura, "Can satellite sensors detect coral reef bleaching? a feasibility study using radiative transfer models in air and water," *Proceedings of the 9th International Coral Reef Symposium*, pp. 1025-1030, 2002.

[15] V. I. Haltrin, "Chlorophyll-based model of seawater optical properties," *Appl. Opt.*, vol. 38, pp. 6826-6832, 1999.

[16] K. Thome, B. Markham, J. Barker *et al.*, "Radiometric calibration of Landsat," *Photogrammetric Engineering and Remote Sensing*, vol. 63, pp. 853-858, 1997.

[17] D. Lirman, and P. Biber, "Seasonal dynamics of macroalgal communities of the northern Florida reef tract," *Botanica Marina*, vol. 43, pp. 305-314, 2000.